

Title: Combined Mesonet and Trackers (UNL Mobile Mesonets)

Authors

University of Nebraska PIs:

Adam Houston, UNL Professor (ahouston2@unl.edu)

Co-Authors:

Kristen Axon, UNL Graduate Student (kaxon2@huskers.unl.edu)

Alex Erwin, UNL Graduate Student (alex.erwin@huskers.unl.edu)

Please contact Adam Houston or Kristen Axon for any data related questions.

Mailing Address: 126 Bessey Hall P.O. Box 880340 Lincoln, NE 68588-0340

CoMeT Overview

The University of Nebraska-Lincoln operates three Combined Mesonet and Tracker (CoMeTs). CoMeTs are Ford Explorers (model years 2015, 2017, and 2019) with forward-mounted suites of meteorological sensors and dual moonroofs, combining the capability of a mobile mesonet to collect near-surface observations with the capability of an unmanned aircraft systems (UAS) tracker vehicle, which enables an observer in the second row of seats to see the aircraft and maintain compliance with Federal Aviation Administration policies on UAS operation. The CoMeTs collect observations of slow temperature and humidity at ~2 m above ground level (AGL) using a Vaisala HMP155A, fast temperature at ~2 m AGL using a Campbell Scientific 109SS-L thermistor, pressure at ~2.5 m AGL using a Vaisala PTB210, wind speed and direction at ~3.25 m AGL using an R.M. Young 05103 propeller anemometer, and vehicle heading using a KVH Industries C-100 fluxgate compass (Barbieri et al. 2019). The HMP155A and 109SS-L thermistor are shielded and aspirated within a U-tube (Waugh and Frederickson 2010; Houston et al. 2016). This list of sensors is also included in the CoMeT data file metadata. Manufacturer specifications for these instruments are given in Table 1 of Hanft and Houston (2018). The reported measured quantities are summarized below. CoMeT-3 was funded through an equipment allocation included in the NSF TORUS award (AGS-1824649).

Instrument Description

The specific sensors included on each CoMeT are summarized in the table at the end of this section. In general each CoMeT collects observations of slow temperature and humidity at ~2 m above ground level (AGL) using a Vaisala HMP155, fast temperature at ~2 m AGL using a Campbell Scientific 109SS-L thermistor, pressure at ~2.5 m AGL using a Vaisala PTB210 barometer with a Gill pressure port, wind speed and direction at ~3.25 m AGL using an R.M. Young 05103 propeller anemometer, position using a Garmin 19x HVS receiver, and vehicle

heading using a KVH Industries C-100 fluxgate compass. The HMP155 and 109SS are shielded and aspirated within a U-tube (Waugh and Frederickson 2010; Houston et al. 2016). Fast temperature and corrected RH measurements (using sensors housed within the U-tube) have a time constant of 10-12 s based on data collected across a temperature and RH shock during the CLOUD-MAP 2017 calibration/validation tests on June 26, 2017. Vehicle speed was < 10 kts for this test.

	CoMeT-1	CoMeT-2	CoMeT-3
Slow Temperature Slow RH	Vaisala HMP155A-L20-PT Part #: 22280-7	Vaisala HMP155E Part #: E1AA11A0B1A1A0A	Vaisala HMP155E Part #: E1AA11A0B1A1A0A
Fast temperature	Campbell Scientific 109SS-L20-PT Part #: 21448-3	Campbell Scientific 109SS-L12-PW Part #: 21448-109	Campbell Scientific 109SS-L12-PW Part #: 21448-150
Pressure	Vaisala PTB-210 Part #: A1A1B Gill Pressure Port Part #: 61002	Vaisala PTB-210 Part #: A1A1B Gill Pressure Port Part #: 61002	Vaisala PTB-210 Part #: A1A1B Gill Pressure Port Part #: 61002
Wind	RM Young 05103-L20-PT Part #: 18435-310	RM Young 05103-L20-PW Part #: 18435-244	RM Young 05103-L20-PW Part #: 18435-244
GPS	Garmin GPS 19x HVS (NMEA 0183) Part #: 010-01010-00	Garmin GPS 19x HVS (NMEA 0183) Part #: 010-01010-00	Garmin GPS 19x HVS (NMEA 0183) Part #: 010-01010-00
Compass	KVH C-100 Part #: 01-0177-15	KVH C-100 Part #: 01-0177-15	KVH C-100 Part #: 01-0177-15
Logger	Campbell Scientific CR6-NA-XT-SW Part #: 28385-9	Campbell Scientific CR6-WIFI-XT-SW Part #: 28385-6	Campbell Scientific CR6-WIFI-XT-SW Part #: 28385-6

Data Collection and Real-Time Processing

The reported measured quantities are summarized in the table below.

Quantity	Units	Source
Epoch time	Seconds	GPS
Latitude and longitude	Degrees	GPS
Altitude	m	GPS
Pressure	hPa	PTB210
Temperature (fast)	deg C	109SS-L
Temperature (slow)	deg C	HMP155

RH (slow)	%	HMP155
Vehicle speed	m/s	GPS
Vehicle heading	deg	C-100 and GPS

In addition to the measured variables, several derived variables are calculated.

Corrected/fast relative humidity (%)

Relative humidity is adjusted to the fast temperature following Richardson et al. (1998) and Houston et al. (2016). This adjustment differs between CoMeT-1 and the other two CoMeTs.

CoMeT-1

Corrected/fast relative humidity is calculated using,

$$RH = 100 \frac{e}{e_s} \quad (1)$$

where vapor pressure and saturation vapor pressure are calculated using the Wexler (1976) formulation fitted by Bolton (1980):

$$e_* = 6.112 \exp \left[\frac{17.67 \cdot T_*}{243.5 + T_*} \right]. \quad (2)$$

For e , the slow dew point temperature (T_{d-slow}) is used for T_* in (2) and is calculated using

$$T_d = \frac{257.14\gamma}{18.678 - \gamma} \quad (3)$$

where

$$\gamma = \ln(0.01 \cdot RH_*) + T_* \frac{18.678 - T_*/234.5}{257.14 + T_*} \quad (4)$$

where slow temperature (T_s) and slow RH_{slow} are used for T_* and RH_* , respectively. For e_s , fast temperature (T_{fast}) is used in (2).

CoMeT-2 and CoMeT-3

As with CoMeT-1, corrected/fast relative humidity uses (1) but dew point temperature is calculated within the logger using

$$T_d = \frac{A_3 \ln \left(\frac{e}{A_2} \right)}{A_2 - \ln \left(\frac{e}{A_1} \right)} \quad (\text{Campbell Scientific manual}) \quad (5)$$

where $A_1 = 0.61078$, $A_2 = 17.558$, and $A_3 = 241.88$ and both e and e_s are calculated within the logger using the expression from Lowe (1977):

$$e_* = B_0 + B_1T + B_2T^2 + B_3T^3 + B_4T^4 + B_5T^5 + B_6T^6 \quad (6)$$

where $B_0 = 6.107799961$, $B_1 = 4.436518521 \times 10^{-1}$, $B_2 = 1.428945805 \times 10^{-2}$,
 $B_3 = 2.650648471 \times 10^{-4}$, $B_4 = 3.031240396 \times 10^{-6}$, $B_5 = 2.034080948 \times 10^{-8}$, and
 $B_6 = 6.136820929 \times 10^{-11}$.

Water vapor mixing ratio (g/kg)

Vapor pressure is calculated using T_{d-slow} as described above and

$$q_v = 62.2 \frac{e}{p}. \quad (7)$$

Dew point temperature (°C)

CoMeT-1

The reported dew point temperature is calculated using (3) and (4) with T_{fast} and RH_{fast} for T_* and RH_* , respectively.

CoMeT-2 and CoMeT-3

The reported dew point temperature is calculated using (6) with T_{slow} to calculate e_s , (7) with RH_{slow} to calculate e , and (5) to calculate T_{d-slow} .

Potential temperature (Kelvin)

$$\theta = T_{fast} \left(\frac{10^5}{p} \right)^{R_d / C_{pd}}$$

Virtual potential temperature (Kelvin)

$$\theta_v = \theta (1 + 0.61 q_v)$$

Equivalent potential temperature (Kelvin)

The expressions use for the calculation of equivalent potential temperature are from Bolton (1980):

$$\theta_e = T_m \exp \left[\left(\frac{3376}{T_{LCL}} - 2.54 \right) q_v (1 + 0.81 q_v) \right]$$

$$T_m = \theta \left(\frac{T_{fast} + 273.15}{\theta} \right)^{0.286 q_v}$$

$$T_{LCL} = 55 + \frac{2840}{3.5 \ln(T_{fast} + 273.15) - \ln(e) - 4.805}$$

Regular intercomparisons between all three CoMeTs were performed during TORUS 2019. Comparisons were also conducted between CoMeT-1 and CoMeT-2 during LAPSE-RATE (2018) on 14 July. In these intercomparisons, the vehicles were parked adjacent to each other aligned perpendicular to (and facing into) the wind. To minimize engine heating effects, intercomparisons were only conducted when the wind speed was >10 kts.

Data Format

Original data files for each deployment are saved as text files and then converted to NetCDF. NetCDF versions have units that are CF compliant and may not match the original units in the txt files. The naming convention for the NetCDF files is as follows:

UNL.CoMeT3.{deployment date YYYYMMDD}.{start time of observation collection in UTC HHMM}.L2.{post-processing codes}.cdf

example: UNL.CoMeT3.20190627.1931.L2.g1.f1.cdf

Post-processing codes are included to track modifications to the raw data. These codes are closely connected to error flags associated with each record. Each letter corresponds to a particular instrument:

- g: GPS
- p: Barometer
- tf: Fast temperature
- ts: Slow temperature
- rh: Relative humidity
- f: Compass
- w: Wind monitor
- a: All instruments

Each number corresponds to a particular post-processing action described more below.

Measured and derived variables are included in the following table.

Variable Heading	Standard Name	Units
time	Time	seconds since 00:00:00, 01-01-1970
Alt	Altitude	meters
lat	Latitude	degrees north
lon	Longitude	degrees east
fast_temp	Air Temperature	kelvin
slow_temp	Air Temperature	kelvin
pressure	Air Pressure	pascals
logger_RH	Relative Humidity	percent

calc_corr_RH	Relative Humidity	percent
wind_speed	Wind Speed	meters per second
wind_dir	Wind From Direction	degrees
vehicle_dir	Vehicle Direction	degrees
dewpoint	Dew Point Temperature	kelvin
mixing_ratio	Humidity Mixing Ratio	g/g
theta	Air Potential Temperature	kelvin
theta_v	Virtual Potential Temperature	kelvin
theta_e	Equivalent Potential Temperature	Kelvin
error_flag		

The error_flag variable is a string that matches the post-processing codes listed above. All instruments will have an associated code, but will have a “0” if the datum is unchanged from the initial processed value.

Error Codes

The following table summarizes the error codes for data collected before 2020:

Error Code	Relevant CoMeT	Description
g1	1,2,3	Exact correction. GPS position and time reprocessed from raw data
g2	1	As far as we can tell this is an exact correction to an error in the GPS time. During the correct time periods the time suddenly went backwards ~250s and stayed at this offset for 750s when it corrected itself. The offset was applied to the “time warp” period.
p1	2	Approximate correction. Hole in the pressure tube connecting the pressure port to the barometer. Resulted in erroneously low air pressure measurements when the vehicle was in motion. Derived variables recalculated (dew point temperature [e depends on qv and p], water vapor mixing ratio, potential temperature, virtual potential temperature, equivalent potential temperature)
a1	3	Exact correction. Missing data reprocessed from raw data

a2	1	Bug fix to bias correction for ts1, ts2, and rh1: water vapor mixing ratio was off by a factor of 10 and virtual potential temperature was wrong because of this.
f1	3	No correction, missing data. Fluxgate compass inoperable. Wind speed and direction calculated using GPS-derived vehicle heading instead.
rh1	1	Approximate correction. Constant bias of +1.7% removed from relative humidity. Derived variables recalculated (corrected/fast relative humidity, dew point temperature, water vapor mixing ratio, virtual potential temperature, equivalent potential temperature)
ts1	1	Approximate correction. Constant bias of +0.6 K removed from slow temperature. Derived variables recalculated (corrected/fast relative humidity, dew point temperature, water vapor mixing ratio, virtual potential temperature, equivalent potential temperature)
ts2	1	Approximate correction. Constant bias of +1.0 K removed. Derived variables recalculated (corrected/fast relative humidity, dew point temperature, water vapor mixing ratio, virtual potential temperature, equivalent potential temperature)

P1 Correction

For the CoMeT-2 data collected during LAPSE-RATE (2018), a hole in the pressure tube required a correction to the pressure and fields derived using pressure. To correct this error, observations from times when CoMeT-1 and CoMeT-2 were in motion and in close proximity were used to evaluate the level of inaccuracy of the CoMeT-2 measurement. Here “close proximity” was defined as any observations within 25 meters of the same point, measured within 90 seconds of one another. The observations with the smallest distance between them were used, and duplicates were removed such that an observation from either vehicle was not used twice. The pressure difference and CoMeT-2 anemometer speed were then aligned with those from CoMeT-1 using a 2nd order polynomial (Fig. 1). Anemometer speed was used instead of vehicle speed because vehicle speed was often a multiple of five, which made it difficult to compute an accurate fit. The polynomial fit was used to calculate a pressure correction for all CoMeT-2 data obtained when the vehicle was in motion and the anemometer speed was greater than 10 m/s.

RH1 Correction

For the CoMeT-1 data collected during TORUS-2019, an approximately constant relative humidity bias of +1.7% was found. This bias was diagnosed using designated intercomparisons between the CoMeTs on 17 May, 18 May, 28 May, 2 June, and 13 June. Focus of the quantification was on comparison to CoMeT-2. As reflected in the table below, RMSE was generally minimized for a correction of 1.7%.

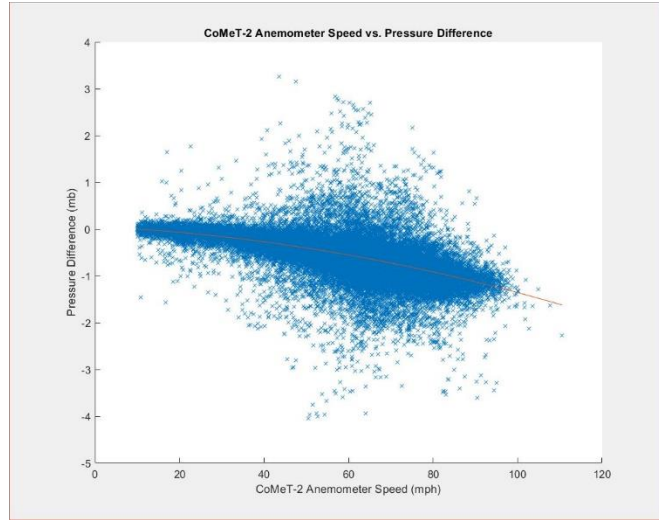
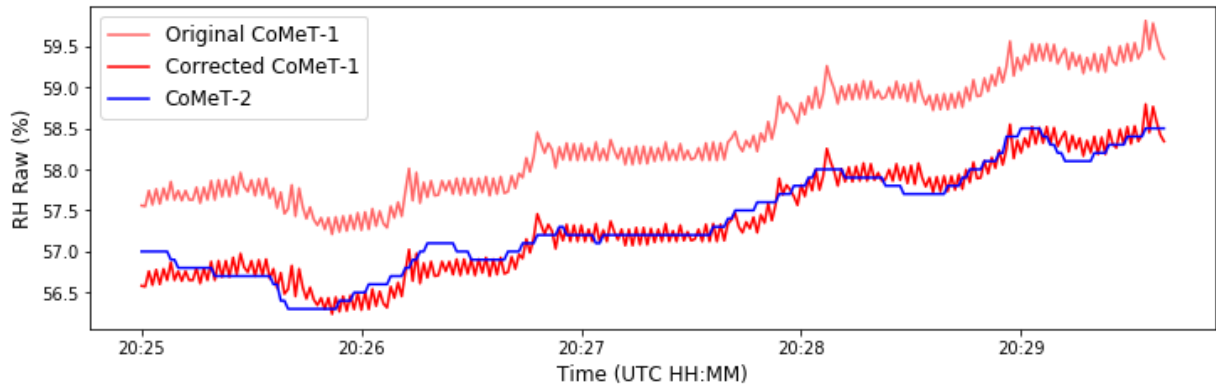


Figure 1. Scatterplot of CoMeT-2 pressure error as a function of anemometer speed. The 2nd-order polynomial fit (red curve) was used for the error correction.

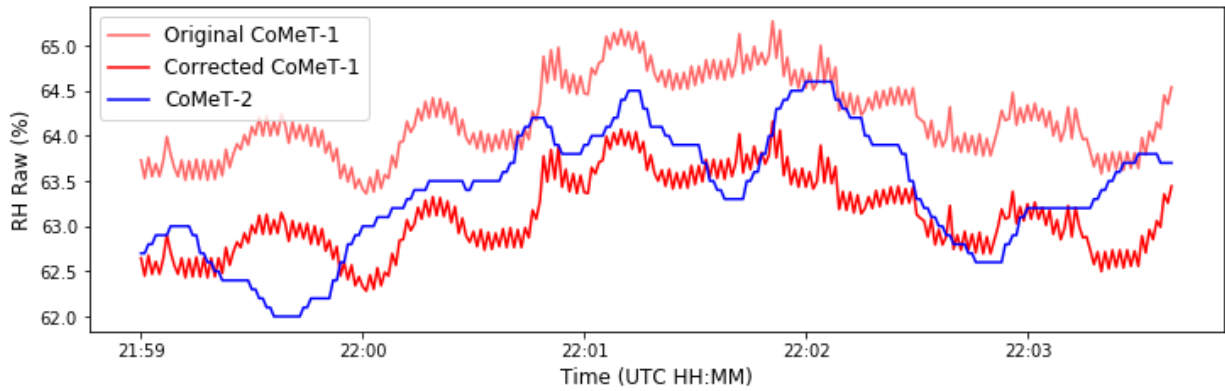
	20190517	20190518	20190528	20190602	20190613
RMSE: 0%	0.99235094	0.97078454	1.0383719	1.4962995	0.87625617
RMSE: 1%	0.42986542	0.54813266	0.6388011	0.95729065	0.54491305
RMSE: 1.2%	0.32634348	0.5205837	0.5930822	0.85445213	0.49146646
RMSE: 1.5%	0.2003671	0.5372993	0.5619939	0.7067458	0.42743146
RMSE: 1.6%	0.17789787	0.55774266	0.5628664	0.6600411	0.41176248
RMSE: 1.7%	0.1730825	0.5845605	0.56945294	0.615086	0.3995384
RMSE: 1.8%	0.18728854	0.6169191	0.58155835	0.5722996	0.39108384
RMSE: 2%	0.2564046	0.6950422	0.6208898	0.49544463	0.3863606

Time series of RH for the five dates shows the improved match to CoMeT-2 relative humidity

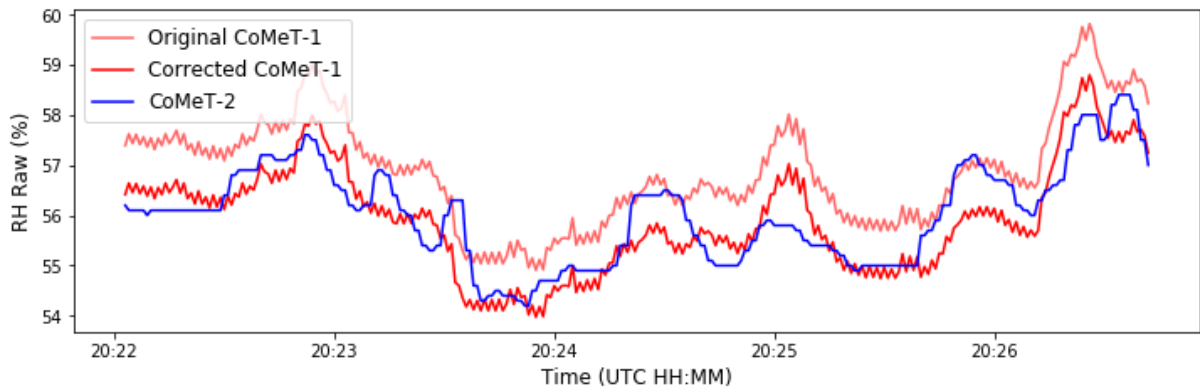
20190517



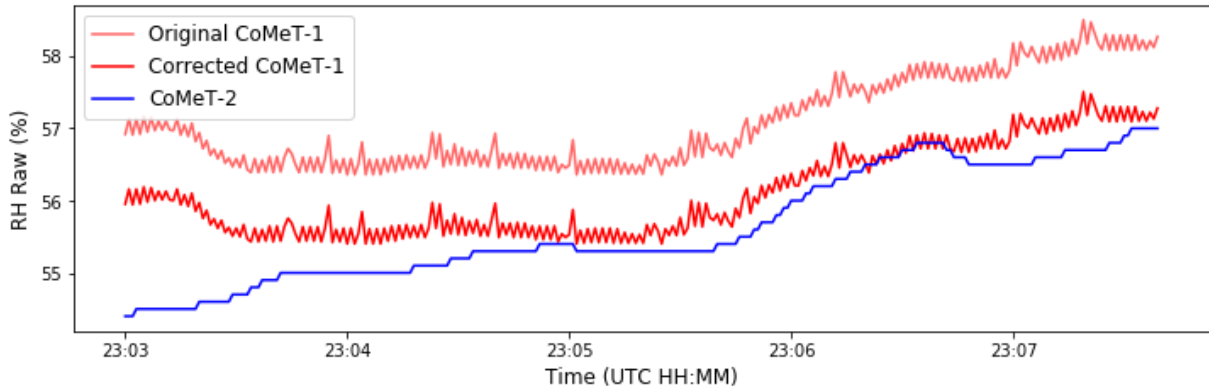
20190518



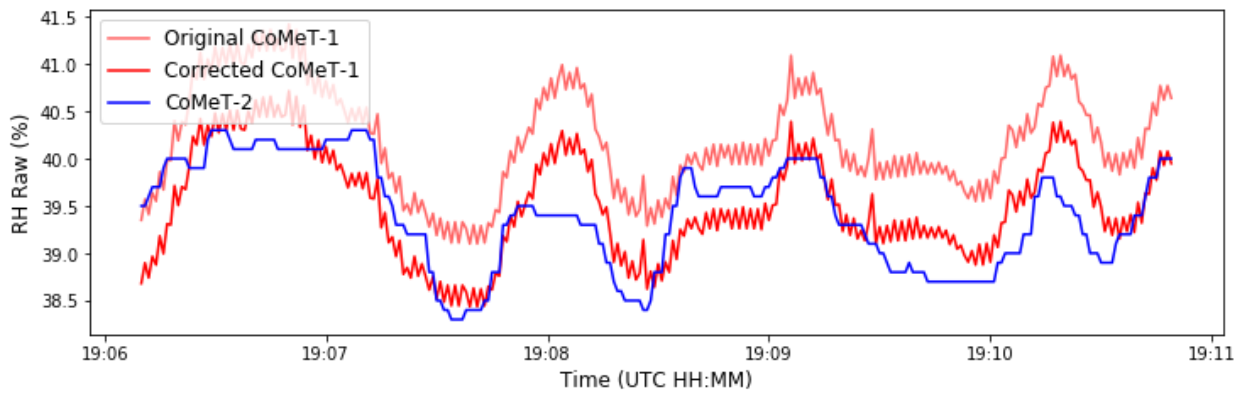
20190528



20190602



20190613



TS1 Correction

	20180714 t1	20180714 t2	20180719
RMSE: 0 K	0.7126725	1.1619352	0.53307545
RMSE: 0.5K	0.3311935	0.7067051	0.22961427
RMSE: 0.6K	0.30007663	0.6239341	0.25774956
RMSE: 0.7K	0.30067468	0.54695326	0.3164639
RMSE: 0.8K	0.33280283	0.4785841	0.39223325

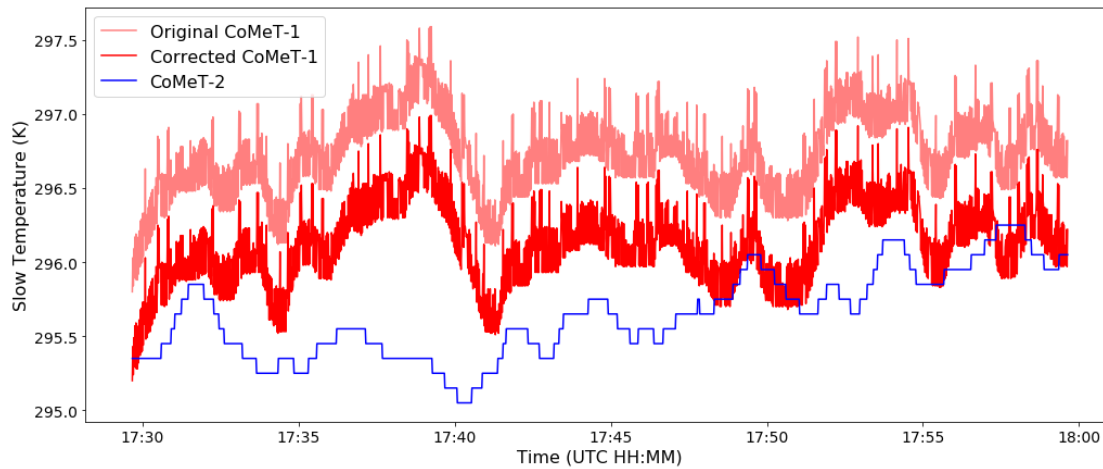
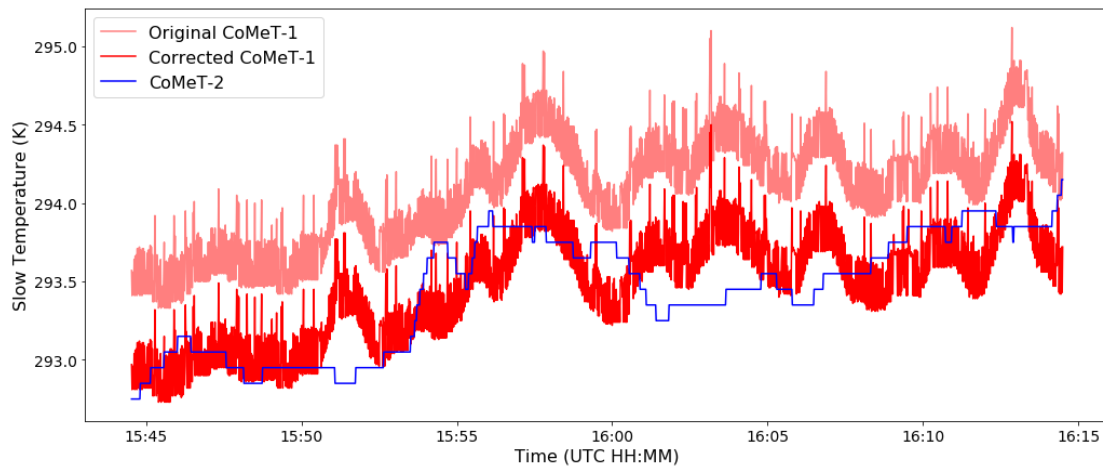
For the CoMeT-1 data collected

RMSE: 0.9K	0.38873616	0.4229724	0.47703278
-------------------	------------	-----------	------------

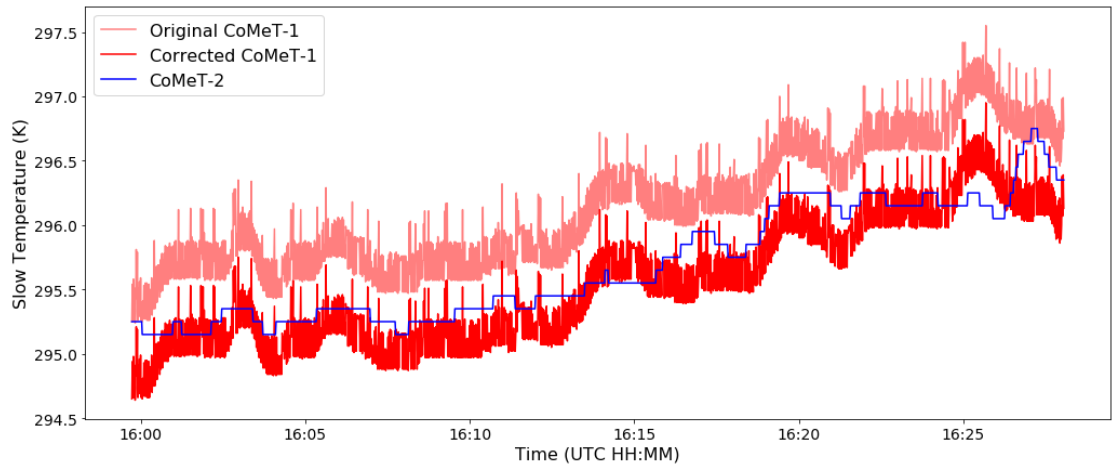
during LAPSE-RATE (2018), an approximately constant slow temperature bias of +0.6 K was diagnosed using designated intercomparison day on 14 July as well as the afternoon data from 19 July. As reflected in the table below, RMSE was generally minimized for a correction of 0.6 K.

Time series of slow temperature for the three time periods shows the improved match to CoMeT-2 slow temperature.

20180714



20180719



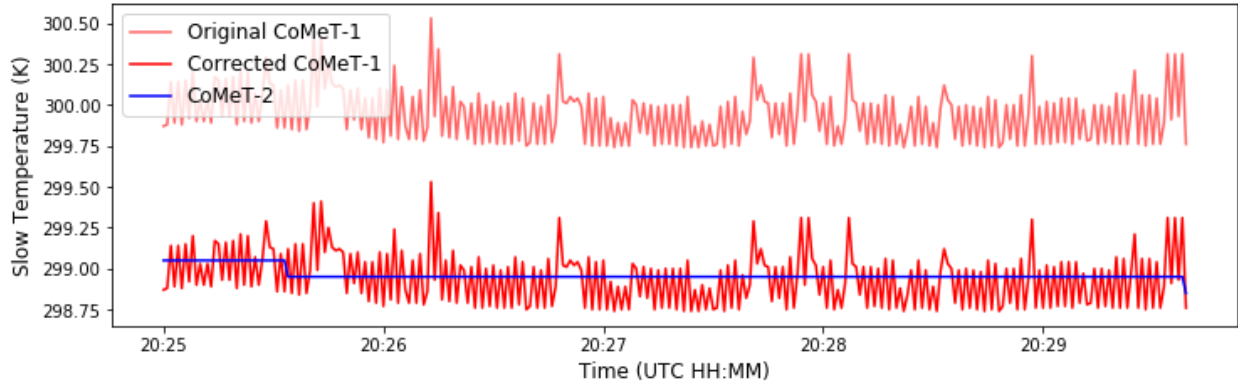
TS2 Correction

For the CoMeT-1 data collected during TORUS-2019, an approximately constant slow temperature bias of +1 K was diagnosed using designated intercomparisons between the CoMeTs on 17 May, 18 May, 28 May, 2 June, and 13 June. Focus of the quantification was on comparison to CoMeT-2. As reflected in the table below, RMSE was generally minimized for a correction of 1 K.

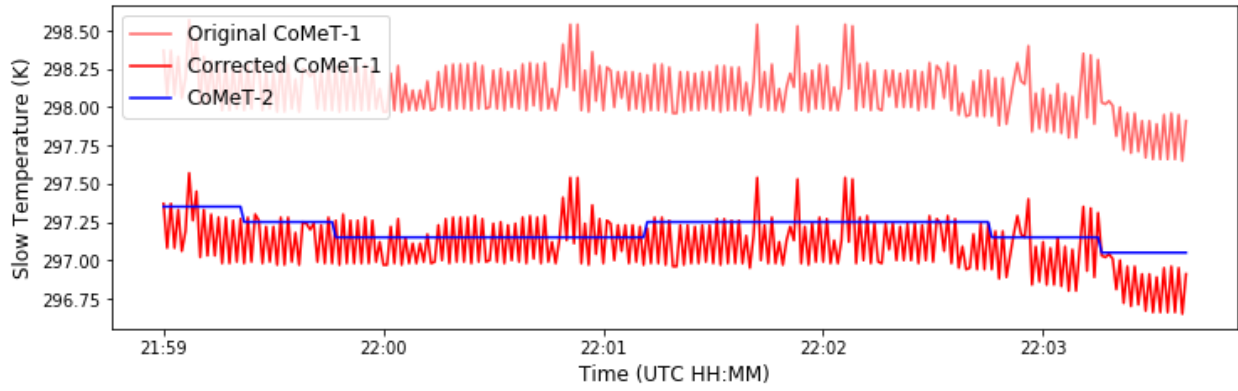
	20190517	20190518	20190528	20190602	20190613
RMSE: 0 K	0.9945115	0.9146924	1.095137	0.8822907	1.0378418
RMSE: 0.8 K	0.24186856	0.19086546	0.3283152	0.21297154	0.27851814
RMSE: 0.9 K	0.17938037	0.16247398	0.24767634	0.20909266	0.20645775
RMSE: 1 K	0.16080011	0.19070503	0.18681198	0.24916872	0.16637215
RMSE: 1.1 K	0.19884285	0.25756836	0.16868997	0.31694293	0.18093376
RMSE: 1.2 K	0.27059698	0.3410527	0.20497885	0.39852604	0.24040964

Time series of slow temperature for the five days shows the improved match to CoMeT-2 slow temperature.

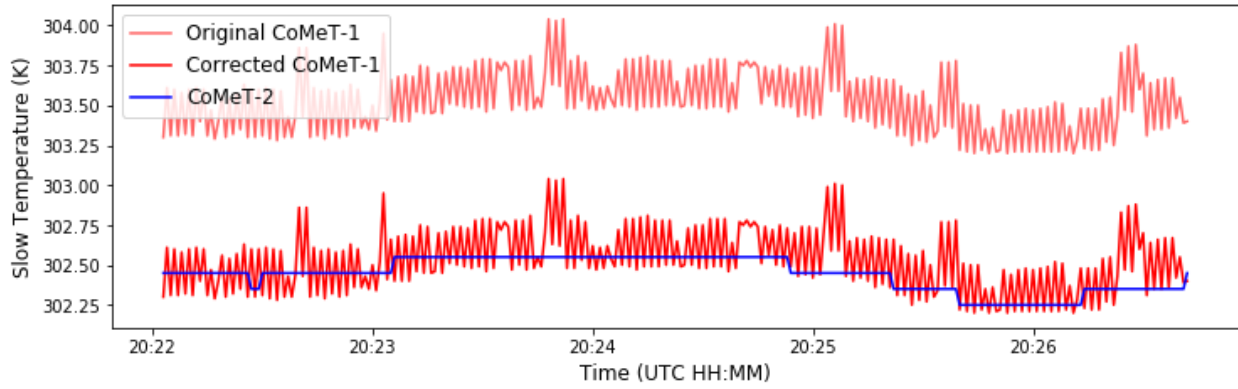
20190517



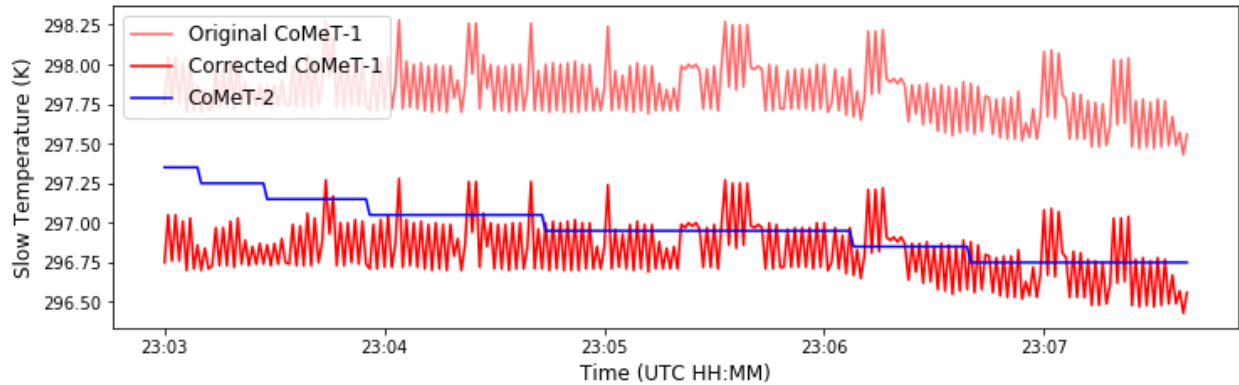
20190518



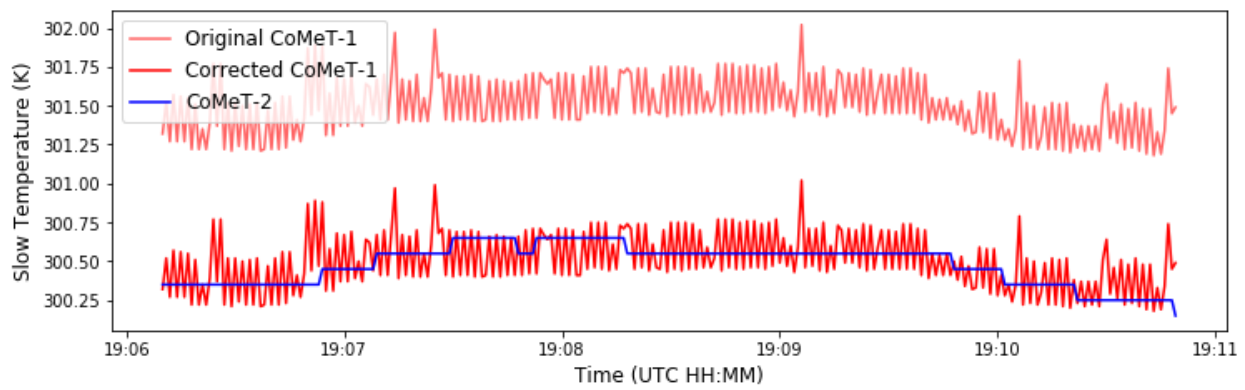
20190528



20190602



20190613



6.0 References

- Bolton, D., 1980: The Computation of Equivalent Potential Temperature. *Mon. Wea. Rev.*, 108, 1046–1053, [https://doi.org/10.1175/1520-0493\(1980\)108<1046:TCOEPT>2.0.CO;2](https://doi.org/10.1175/1520-0493(1980)108<1046:TCOEPT>2.0.CO;2).
- Hanft, W., and A. L. Houston, 2018: An Observational and Modeling Study of Mesoscale Air Masses with High Theta-E. *Mon. Wea. Rev.*, 146, 2503–2524, <https://doi.org/10.1175/MWR-D-17-0389.1>. Wexler
- Houston, A. L., R. J. Laurence III, T. W. Nichols, S. Waugh, B. Argrow, and C. L. Ziegler, 2016: Intercomparison of unmanned aircraft-borne and mobile mesonet atmospheric sensors. *Journal of Atmospheric and Oceanic Technology*. 33, 1569-1582, doi: 10.1175/JTECH-D-15-0178.1.
- Lowe, P. R., 1977: An Approximating Polynomial for the Computation of Saturation Vapor Pressure. *J. Applied Meteorology*, 16, 100–103.
- Richardson, S. J., S. E. Frederickson, F. V. Brock, and J. A. Brotzge, 1998: Combination temperature and relative humidity probes: Avoiding large air temperature errors and associated relative humidity errors. Preprints, 10th Symp. On Meteorological Observations and Instrumentation, Phoenix, AZ, Amer. Meteor. Soc., 278–283.
- Waugh, S., and S. E. Frederickson, 2010: An improved aspirated temperature system for mobile meteorological observations, especially in severe weather. 25th Conf. on Severe Local

Storms, Denver, CO, Amer. Meteor. Soc., P5.2. [Available online at https://ams.confex.com/ams/25SLS/techprogram/paper_176205.htm.]